

Aqueous foam slip and shear regimes determined by rheometry and multiple light scattering

Sebastien Marze and Dominique Langevin

Laboratoire de Physique des Solides, CNRS UMR 8502, Université Paris-Sud, Orsay, France

Arnaud Saint-Jalmes^{a)}

Institut de Physique de Rennes, CNRS UMR 6521, Université Rennes 1, Rennes, France

(Received 21 August 2007; final revision received 26 March 2008)

Synopsis

By using simultaneously rheometry and a multiple light scattering technique, diffusing wave spectroscopy (DWS), we have studied the steady flows of three-dimensional aqueous foams. A number of parameters—the surfactants, the liquid volume fraction, and the roughness of the rheometer surfaces—are widely varied in order to determine which quantities have an impact on the macroscopic flow behaviors. By comparing to previous theoretical and experimental results, we show that flow regimes can either be slip or shear dominated. Two opposite slip regimes are identified; the transition from one to the other is obtained either by changing the surfactant or the liquid fraction, and we quantitatively discuss which regime is selected for any given foam properties. Similarly, different shear regimes are also found, and we discuss the link between the macroscopic rheometry measurements, the nature of the flow, and the interfacial microscopic properties. Despite the occurrence of slip, we show how we can recover the actual shear rate by DWS, and how we can quantitatively explain the measured slip velocities. © 2008 The Society of Rheology. [DOI: 10.1122/1.2952510]

I. INTRODUCTION

Aqueous foams are parts of our everyday life. On one hand, we use them a number of times per day in various environments, often in contact with our bodies, or even eating them. On the other hand, industrial processes, such as froth flotation, demand a huge volume of aqueous foam. In both cases, foams often undergo stresses that can lead them to flow. Thus, it is important to understand the flow properties of aqueous foams, in order to optimize industrial procedures, or to conceive new applications and materials.

A large amount of foam rheological studies have focused on the linear viscoelasticity and yielding, evidencing some universal features once rheological quantities are normalized by the Laplace pressure $P = \sigma/R$, with σ the gas-liquid surface tension, and R a characteristic bubble dimension [compilations of results can be found in Rouyer *et al.* (2005) and Höhler and Cohen-Addad (2005)]. Comparatively, there are fewer studies on

^{a)}Author to whom correspondence should be addressed; electronic mail: arnaud.saint-jalmes@univ-rennes1.fr

the steady flow of foams. In fact, many experimental and theoretical results are reported on the flow of two-dimensional (2D) foams [Kraynik *et al.* (1991); Tewari *et al.* (1999); Debrégeas *et al.* (2001); Asipauskas *et al.* (2003); Janiaud and Graner (2005); Cantat and Delannay (2005); Janiaud *et al.* (2006); Wang *et al.* (2006); Cox (2006); Dollet and Graner (2007)]. A 2D foam consists of only one layer of bubbles, usually constricted between glass plates. Such systems are actually quite useful to approach foam flows: One can always see all the bubbles, their deformations, or the velocity field. However, a major drawback with 2D foams is the central role of the friction of the bubbles on the supporting plates. This friction is dominating all the other viscous effects, and different results can be found by changing the experimental setup [Wang *et al.* (2006)]. Thus, despite important insights that can be evidenced with 2D foams (for instance, on the nature and statistics of plastic events during flow or on the occurrence of strain localization) these studies cannot be transposed in a straightforward way to model the flow of three-dimensional (3D) foams.

With 3D foams, the different experimental or theoretical results reported [Khan *et al.* (1988); Princen and Kiss (1989); Reinelt and Kraynik (1993); Gopal and Durian (1999); Bertola *et al.* (2003); Rodts *et al.* (2005); Denkov *et al.* (2005)] did not get a clear picture of the steady flow properties, especially regarding the flow uniformity. Indeed, with 3D foams (which are opaque), it is almost impossible to monitor the flow in bulk. So, nonuniformities like shear banding or strain localization are not easy to evidence. Recently, by coupling rheometry and nuclear magnetic resonance (NMR) experiments Raynaud *et al.* (2002) and Bertola *et al.* (2003) measured bulk velocity profiles, and showed that nonuniform flows can actually occur. However, with transparent (density matched) emulsions, it has also been shown that the occurrence of shear banding depends on the chemical formulation and on the interactions between the droplets [Bécu *et al.* (2006)]. Today, it turns out that the important parameters, on which the flow properties depend, are still not well identified.

Also, the possible occurrence of slip on the surfaces of the rheometer and its impact on the flow properties are still not completely understood for aqueous foams. Many recent works have focused on these slip issues, implementing the seminal works of Bretherton (1961), and trying to deepen our understanding of the hydrodynamics within the liquid layers separating the bubbles and the walls [Denkov *et al.* (2005, 2006); Terriac *et al.* (2006); Saugey *et al.* (2006); Emile *et al.* (2007)]. The existing models predict that different slip regimes can be obtained depending on an interfacial “mobility” (controlled by the surfactants adsorbed at the interfaces) and on the liquid volume fraction. Different power laws between the slip velocity and the stress characterize these regimes. Today there are some experimental results reported on the exponents of these laws, but much less on the prefactors, and a complete quantitative model including all the effects is still lacking. It is finally also important to test the universality of the results, and whether the flow of foams is similar to the ones of other soft materials like emulsions, microgels, or even granular matter. More information is thus needed to better figure out the links between the flow uniformity, the slip, and the chemicals and interfacial properties.

The purpose of this article is to present new experimental data on flow of 3D aqueous foams based on several surfactants, different liquid volume fractions, and for different roughness conditions applied to the rheometer surfaces. Our measurements are made with a careful control of the foam physical and chemical properties, especially allowing us to correctly manage the undesired aging affects. Simultaneously, a light scattering technique, diffusing wave spectroscopy (DWS), probes the dynamics of the elementary bubble rearrangements, which can then be linked to the macroscopic results.

The article is written as follows: Sec. II presents the different chemicals (with the

interfacial properties) and methods; the raw results of rheology and DWS are given in Sec. III for the different surfactant systems, liquid fractions, and roughness conditions. All these results are analyzed in Sec. IV, with comparisons to previous models and results on foams and on other soft materials.

II. MATERIALS, METHODS AND ANALYSIS

A. Foam production and materials

The foams are produced by using a turbulent mixer apparatus [Saint-Jalmes *et al.* (1999a)]. The principle consists of injecting the solution and the gas, at high pressures, inside a T junction. In the middle of the T , the diameter of the liquid channel is strongly reduced, down to 0.7 mm in order to create a high-speed jet, to which the gas is added. The mixture hence flows in a turbulent regime along a final hose, providing homogeneous foams with bubble radius of $70 \pm 10 \mu\text{m}$ (measured at the surface of samples by optical transmission microscopy) depending on the foaming chemical. The liquid volume fraction ε , controlled by adjusting the gas and liquid flow rates in the foam generator, is varied from 0.05 up to 0.25 in this study. For the gas, we use perfluoroethane (C_2F_6): it has low diffusion and solubility constants, considerably limiting coarsening and drainage of the foams [Saint-Jalmes (2006)]. Three types of foaming chemicals are used: Sodium dodecyl sulfate (SDS), an anionic surfactant; casein (CAS), a mixture of milk proteins; and Amilite GCK-12 (GCK), a commercial name for an anionic surfactant made of a fatty acid residue from coconut oil. The first two were sold by Sigma-Aldrich and the third was kindly provided by Ajinomoto Co., Inc. For these chemicals, the concentrations used are respectively $C_{\text{SDS}}=6 \text{ g l}^{-1}$, $C_{\text{CAS}}=4.5 \text{ g l}^{-1}$ and $C_{\text{GCK}}=10 \text{ g l}^{-1}$. The casein solution is brought at pH 5.6 by adding a phosphate buffer at 10 mM, and then placed in an ultrasonic bath for 30 min, so as to prevent casein from aggregating during the dissolution. The solution is then stirred at 1000 rpm during 8 h. After this procedure, the CAS solution can be used for two days, before bacteria development. For GCK, the solution pH is 8.2.

Adding the chemicals to water does not change the bulk viscosity η , which remains quite close to 1 mPa s. The surface tensions σ are 36, 22, and 46 (± 0.5) mN m^{-1} , respectively, for SDS, GCK, and CAS (measured by the rising bubble method). An equilibrium value is reached within 1 min after the formation of the bubble for SDS and GCK. For CAS, a slow drift is still observed after 10 min (due to protein reorganization at the surfaces). We use the value at a typical instant of 300 s, which corresponds to the mean duration of a rheology or DWS measurement.

We have selected these chemicals to be sure that very different behaviors at the gas-liquid interfaces and in thin films separating the bubbles are obtained. With SDS, the interfaces are fluid like, and the films are flat, uniform, with a typical thickness of a few tens of nm. The GCK foams have similar types of films, but the interfaces are much more viscous and elastic. On the other limit, the use of casein creates highly viscoelastic interfaces [Bos and van Vliet (2001)]; moreover, the films are very peculiar: they are thick (hundreds of nm) and appear as gelified, and nonuniform in thickness (due to the confinement in the film of large protein aggregates) [Saint-Jalmes *et al.* (2005)]. If the interfacial properties have an impact on the macroscopic foam flow, we can then expect to evidence it with such different systems.

B. Rheometry

Measurements are performed with a MCR 300 Rheometer, from Anton Paar. The foams are studied using homemade cone-plate geometries in Plexiglas (cone diameter

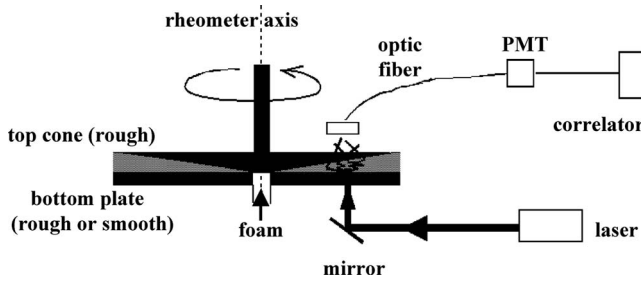


FIG. 1. Experimental setup consisting of a cone-plate rheometer coupled to a DWS setup (in transmission mode). The cone surface of the rheometer cone is always rough, while we use either a smooth or a rough surface for the bottom plate. The foam is injected inside the cell at the center, from below.

= 175 mm, angle = 0.175 rad). The cone is always covered with polydisperse sand grains having a mean diameter around 100 μm . The bottom plate is used with or without glued grains, in order to get a smooth or a rough surface (Fig. 1).

We performed experiments at controlled shear rates $\dot{\gamma}$, varied typically from 10^{-3} to 15 s^{-1} . For higher rates, the sample is ejected out of the cell. In the purpose of implementing the steady shear data at high shear rates, we also performed oscillatory strain sweeps at different fixed frequencies, from 0.3 up to 9 Hz. The oscillatory strain amplitude is swept from 0.01 up to 2. In that way, we can theoretically get similar and even higher shear rates than with the steady-shear mode; the validity of this approach will be discussed in Sec. III.

Practically, a complete flow curve can be obtained on a single sample. However, with the shear rates range investigated and to get enough points on the curve, this leads to more than a few minutes of measurement time. Moreover, the light scattering technique (DWS, see below) also requires a few minutes in order to average the temporal fluctuations of intensity. So, a 10-point flow curve would need at least 10 min to be measured. This is too long for a single foam sample, especially at high liquid volume fractions where significant aging may occur between the first and last points. This is why shear stresses are measured independently on different samples, only one shear rate being applied to a given foam. The results shown on the plots are then averaged over a few samples (3–4) for each shear rate. Moreover, for each shear rate, the plotted stress is the constant value found in the steady state (although the onset of this regime depends on the shear rate, it is commonly set at a shear strain of 100%). Note also that as the foam sample height in the rheometer is small when compared to the usual liquid capillary holdup length (corresponding to the height of the wet layer at the bottom of a foam and inversely proportional to the bubble size [Saint-Jalmes (2006)]), wet foams can be studied without fast and significant drainage.

C. Diffusing wave spectroscopy (DWS)

A diffusing wave spectroscopy (DWS) setup is coupled with the rheometer (Fig. 1). A highly coherent monochromatic laser at $\lambda = 532 \text{ nm}$ is used for the light source, the transmitted light is then collected by an optic fiber, and directed towards a photon counting detector, finally feeding a correlator. Note that the sand did not prevent the experiment: The cone and plates remain always sufficiently transparent. DWS allows us to measure a typical time scale associated with the dynamics inside the foam; this dynamics is either induced by the applied shear, or by the foam coarsening [Durian *et al.* (1991); Gopal and Durian (1999); Höhler and Cohen-Addad (2005)]. The formalism and its

application for colloidal particles and foams has been described in Weitz and Pine (1993) and Durian (1995). From the intensity variations $I(t)$, one first calculates the intensity autocorrelation function; this function is related to the electrical field autocorrelation function $g_1(t)$ (Siegert relation):

$$\frac{\langle I(0)I(t) \rangle}{\langle I \rangle^2} = 1 + \zeta |g_1(t)|^2 \quad (1)$$

ζ is an experimental factor depending on the optical setup characteristics, ranging from 0.1 to 0.9 [Weitz and Pine (1993)]. For aqueous foams, $g_1(t)$ has been calculated, in transmission [Durian *et al.* (1991)]:

$$g_1(t) = \frac{(L/l^*)\sqrt{6(t/T)^n}}{\sinh[(L/l^*)\sqrt{6(t/T)^n}]}, \quad (2)$$

where L is the sample thickness; T is the characteristic time of the foam dynamics, and l^* is the transport mean free path of light. The latter is related to the bubble size [Vera *et al.* (2001)]. When the dynamics is due to uncorrelated events, like for coarsening, $n=1$ and T corresponds to the averaged time between rearrangement events at a given location in the sample; whereas $n=2$ implies a continuous and convective bubble motion [Wu *et al.* (1990); Gopal and Durian (1999)].

As schematized in Fig. 1, the laser spot hits in the middle of the cone radius, about 43 mm from its center. At this position, the sample thickness is approximately 7 mm $\gg l^*$. The smallest L/l^* ratio, obtained for the lowest liquid volume fraction (0.05) has a value of 12 and is sufficient to be in the multiple light scattering limit and to use the DWS formalism.

III. RESULTS

A. SDS foams

1. Rheometry results

Figure 2 presents the flow curves (stress τ , derived from the measured torque, as a function of the shear rate $\dot{\gamma}$) obtained for SDS foams at a liquid fraction $\varepsilon=0.15$, with the two different plate roughness conditions. It turns out that the roughness of the plate is clearly important and that the flow curve depends strongly on this experimental condition. For all values of ε , the same qualitative trends are observed and only the stress range decreases with the liquid fraction, as shown below.

We first describe in more detail the flow curves obtained with a rough bottom plate, and as a function of the liquid fraction (Fig. 3). On this plot, we have compiled the steady-shear data and the points obtained by oscillations: The latter correspond to measurements at various frequencies, but at a constant amplitude γ of 100%, in order to get the same value for the shear rate and for the frequency ω ($\omega = \dot{\gamma}/\gamma$). Using this method, we find that the points collected by oscillations agree with those of steady shear (except for the wettest foam, where stability issues of drainage can be important). This allows us to implement the range of accessible shear rate; in the same time, this seems to be a first proof that the Cox–Merz rule holds for aqueous foams; but note though that this is found over less than a decade in frequency or shear rate, and this has to be investigated in more detail.

Concerning the shape of the flow curves, whatever the liquid fraction, we identify a typical yielding behavior, with a nonzero limit of the stress at low shear rate corresponding to a yield stress, τ_y . Such flow data can actually be adjusted with a Herschel–Bulkley

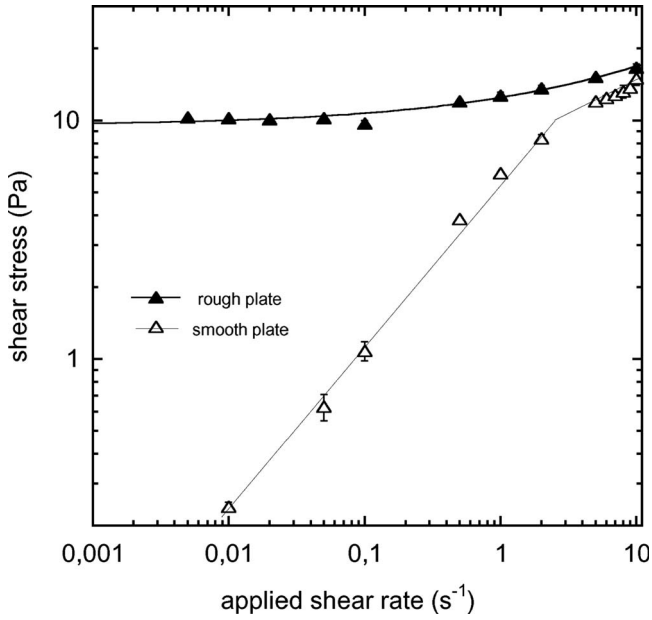


FIG. 2. Flow curves—shear stress τ as a function of the applied shear rate—for SDS foams at $\epsilon=0.15$. Effect of the roughness: Full symbols correspond to a rough plate, and open symbols to a smooth plate.

(HB) model: $\tau = \tau_y + \alpha_v \dot{\gamma}^\beta$ (α_v has the dimension of a consistency), as shown by the solid lines in Fig. 3, left. As the liquid fraction increases, the whole curve is shifted downward, but the exponent remains constant: We find $\beta = 0.42 \pm 0.02$. Another way to present such a behavior is to focus on the high shear rates and to plot the viscous stress $\tau_v = \tau - \tau_y$ as a function of $\dot{\gamma}$, for the different liquid fractions. One directly visualizes scaling regimes (Fig. 3, right), with an exponent $\beta = 0.42 \pm 0.02$.

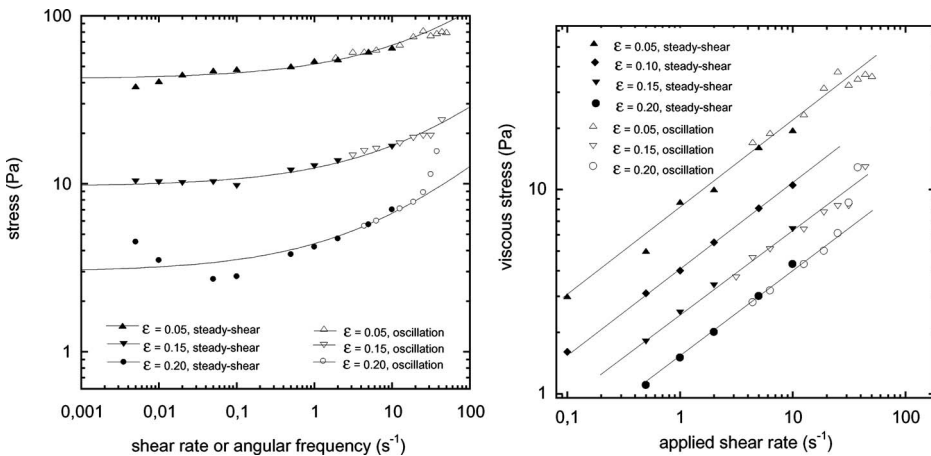


FIG. 3. (Left) Flow curves for SDS foams, at various liquid fractions: Including both measurement obtained during steady shear and measurements during oscillations (at various frequencies ω , for a fixed strain amplitude of 1). Solid lines are fits based on the Hershel–Bulkley (HB) models. (Right) Viscous shear stress, $\tau_v = \tau - \tau_y$, vs applied shear rate for different liquid fractions. Lines are power law fits, with a constant exponent $\beta = 0.42$.

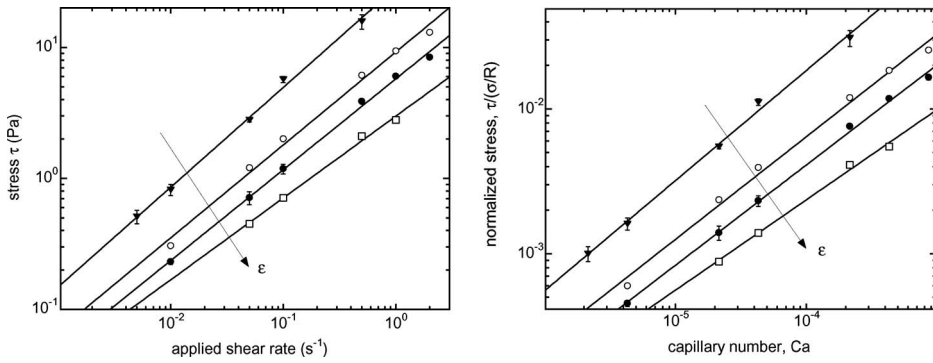


FIG. 4. (Left) Shear stress τ vs applied shear rate for SDS foams on a smooth plate ($\varepsilon=0.2, 0.15, 0.1$ and 0.05). Here only the first regime is shown ($\tau < \tau_y$). (Right) Same data in a nondimensional form: Normalized slip stress $\tau' = \tau / (\sigma/R)$, calculated by integrating the stress along a radius, as a function of the dimensionless capillary number Ca defined in the text.

For the flow curves with a smooth bottom plate and for all the liquid fractions, it is impossible to determine a yield stress: Stresses continuously decrease with decreasing shear rates $\dot{\gamma}$, and can be at least one order of magnitude lower than with a rough plate. At a critical rate $\dot{\gamma}_c$, a kink is well evidenced, separating two regimes. In fact, this slope rupture always occurs precisely at the yield stress value seen for the rough conditions. The first regime can be characterized by a power law behavior $\tau = \alpha_s \dot{\gamma}^\delta$ (up to $\dot{\gamma}_c$). The liquid fraction dependence of this first regime is shown in Fig. 4, left. The exponent δ is independent of the liquid fraction and equals 0.65 ± 0.01 .

Concerning the high shear rates range, the behavior seems to follow another power law behavior, but there are not enough points to determine it precisely. However, it is always observed that shear stresses with either smooth or rough plates meet at the highest shear rates.

2. DWS results

Typical data for a SDS foam at $\varepsilon=0.15$ for the rough and smooth plates are shown in Fig. 5. We have plotted $1/T$ as a function of $\dot{\gamma}$, with T deduced from the intensity autocorrelation curves as discussed in Sec. II.

First, note that for a quiescent foam (at $\dot{\gamma}=0$), the gas diffusion from bubbles to bubbles creates both an increase of the mean bubble size (coarsening) and some bubble rearrangements (side swapping, also known as “T1”). In this case, the DWS data—for which $n=1$ to fit the data—provide us with the rate of coarsening-induced rearrangements.

Under shear and with rough surfaces, we find that the autocorrelation curve fits are always better using $n=2$, rather than 1. Continuous shear-induced flows are thus dominating over coarsening rearrangements. Note that this fitting procedure with $n=2$ is less efficient for the lowest shear rate, where a contribution of discrete shear-induced rearrangement ($n=1$) should probably be added; however, it remains clear that the main mechanism is the one corresponding to $n=2$, and we will only keep this one for all the shear rates. In this regime, we find that the dependence of $1/T$ with shear rate follows a power law with an average exponent of 0.80 ± 0.05 . The exponent is independent of the liquid volume fraction, and the prefactor decreases with the liquid volume fraction. A closer look shows that the exponent is actually close to 0.9 at the lowest $\dot{\gamma}$, and slightly decreases at high $\dot{\gamma}$.

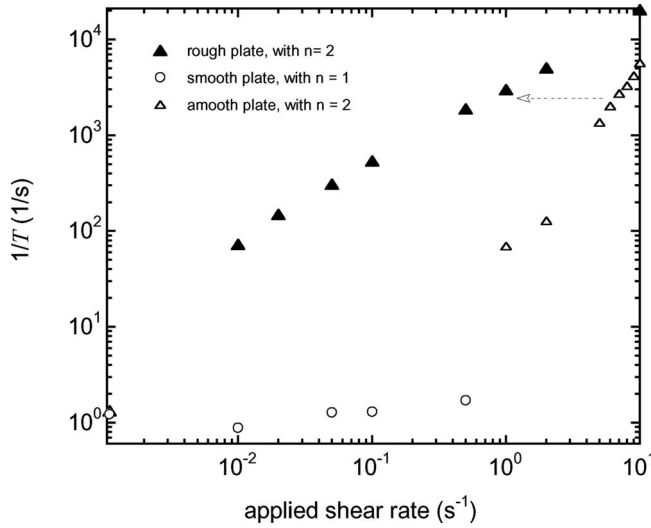


FIG. 5. Typical DWS results for SDS foams at $\varepsilon=0.15$: Rearrangement frequency ($1/T$) vs applied shear rate on a rough plate (filled symbols) and on a smooth plate (open symbols), averaged on 3–4 measurements for each applied shear rate. The circles correspond to $n=1$ and the triangles correspond to $n=2$ [see Eq. (2)].

For the smooth plate at low shear rates, we get a plateau, which turns out to be exactly at the same value as the one for a foam at rest; along this plateau, data fitting is always better using $n=1$. Above a critical shear rate, which corresponds to the same $\dot{\gamma}_S$ identified in the flow curve, another power law is found, with an exponent of 1.75 ± 0.25 that does not depend on the liquid volume fraction either. Note that $1/T$ is always smaller than the one measured with rough plates. Nevertheless, at the highest shear rates, $1/T$ no longer depends on the roughness. These results are consistent with previous published results [Gopal and Durian (1999)], and will be discussed in Sec. IV.

B. Casein foams

1. Rheometry results

In Fig. 6, flow curves for CAS foams at $\varepsilon=0.15$, with smooth and rough plates, are shown. For rough plates, a shape consistent with a HB behavior (solid line) is found; however, the yield stress appears less marked. The high shear rates regime is described by a power law with an exponent β of 0.30 ± 0.01 . For the opposite case of the smooth plate, the flow curve at low shear rates gives a power law with an exponent δ of 0.32 ± 0.01 . There is only a tiny change of slope at the yield stress, and at the highest shear rates, an exponent still quite close to 0.3 can be estimated.

The comparisons between SDS and CAS foams are summarized in Fig. 7: it is clearly shown that the surfactant and thus the interfacial and film properties control both the slip and the shear behaviors.

2. DWS results

Qualitatively, the results are similar to the ones of SDS foams. With a rough plate, $1/T$ follows an almost linear behavior, using $n=2$. While with a smooth plate, a first plateau is observed (with a fitting parameter $n=1$) corresponding again to the value at $\dot{\gamma}=0$. For high shear rates, a power law is found with the same exponent as for the SDS foams.

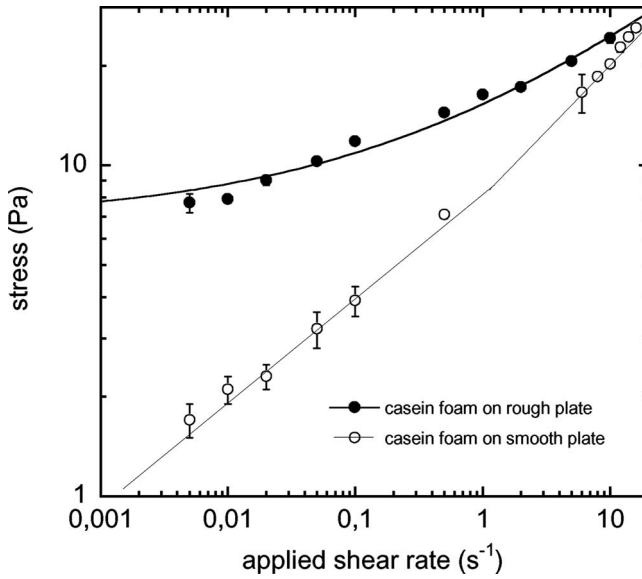


FIG. 6. Flow curves for CAS foams at $\varepsilon=0.15$ and effect of the roughness. Full symbols for a rough plate and open symbols for a smooth plate.

C. GCK foams

For GCK foams, only flow curves have been measured, for both plate roughness and several liquid volume fractions ε up to 0.25. A HB behavior is well evidenced, as for SDS, with rough surfaces, allowing us to determine the yield stresses. For the high shear rates, the exponent β has a unique value of 0.49 ± 0.01 , whatever ε .

With the smooth plate, a more complex behavior than with SDS and CAS is observed for the low shear rates, corresponding to stresses below the yield stress τ_y . Oppositely to SDS and CAS, there is not only one single power law behavior (Fig. 8) over the whole range of $\dot{\gamma}$. In fact, we can still find a range of shear rates where the exponent δ can be determined as previously (solid lines on Fig. 8), up to a $\dot{\gamma}_s$ for which $\tau = \tau_y$. But, first, this exponent turns out not to be constant: it increases with the liquid fraction, $\delta=0.28, 0.44$,

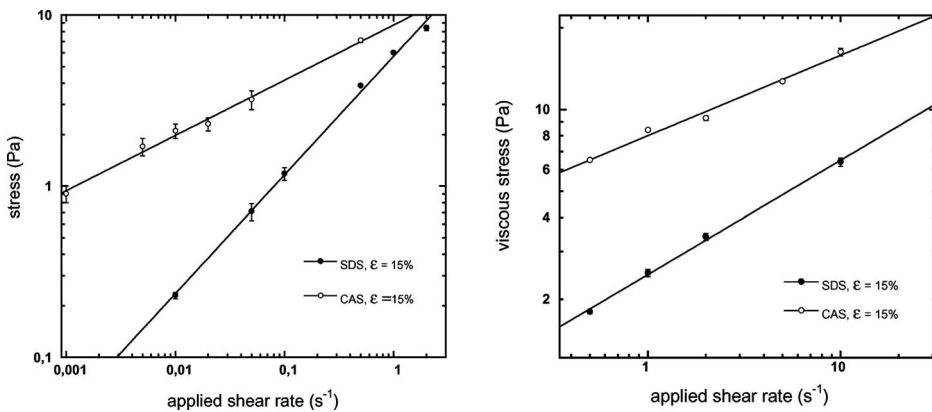


FIG. 7. Comparisons between SDS foams and CAS foams: (left) first regime with a smooth bottom surface ($\tau < \tau_y$), and (right) viscous stress τ_v , with a rough bottom surface.

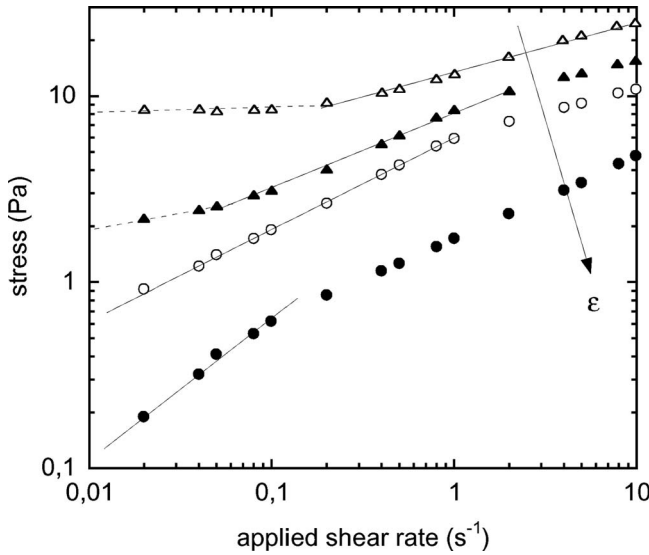


FIG. 8. Flow curves for GCK foams, at various liquid fractions ($\varepsilon=0.2, 0.15, 0.1,$ and 0.05) and with a smooth bottom plate.

0.48, and 0.66 for $\varepsilon=0.05, 0.10, 0.15,$ and 0.25 respectively. Second, another behavior is found at very low shear rates. Another power law is more and more evidenced as the foam is dry (dashed lines in Fig. 8): Its exponent decreases almost down to zero and the corresponding range of shear rates increases as ε decreases.

IV. DISCUSSION

A. Slip or shear: DWS data analysis

First, we show that the coupling of DWS and rheometry can provide us with the type of flow occurring in the foam, whatever the roughness and the shear rates. In one hand, with rough surfaces, a uniform flow without slip can be expected. According to Gopal and Durian (1995), under such conditions, the rate of rearrangements $1/T$ inside the foam is simply linear with the shear rate. Such linear relationship was also found with laminar shear flow of dilute colloidal suspension [Wu *et al.* (1990)]. For aqueous foams, this linearity and quantitative agreement have also been found experimentally in a cylindrical Couette rheometer by Gopal and Durian (1999). In that context, the power law we find, with an exponent slightly below 1, is consistent with previous works. However, the smaller value measured implies some disturbing phenomena, most likely some slip occurring at the highest shear rates. This means that with rough surfaces, as initially expected, there is mostly no slip (unless at the highest shear rates). It is interesting to note that the existence of slip does not only depend on the plate roughness itself, but also on the applied shear rate.

In the other hand, for the smooth plate, using the DWS data, we can determine that the low shear rates regime (before $\dot{\gamma}_s$) is a pure slip behavior: The constant value of $1/T$ —equal to the value found for foams at rest—and $n=1$ prove that the foams actually slip on the smooth plate without any shear-induced bubble rearrangements. The foam translation due to slip is actually not fast enough, when compared to the coarsening

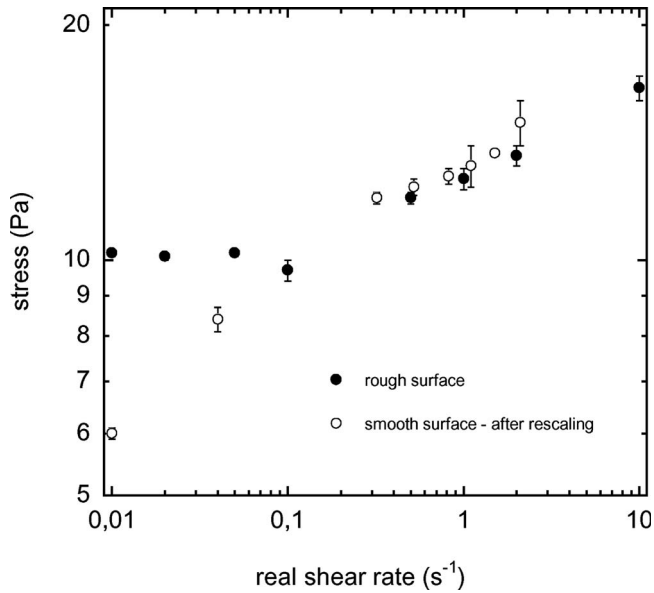


FIG. 9. Flow curves for rough and smooth plates (SDS foam at $\varepsilon=0.15$), as a function of the *real* shear rate deduced from the DWS measurements. For the smooth plate, only the points above the yield stress, where shear occurs simultaneously to slip, have to be considered in this graph.

dynamics, to be responsible for the decorrelation of light: Thus this translation has no effect on the DWS data, as if the foam stays at rest, only subjected to coarsening-induced rearrangements.

Above $\dot{\gamma}_S$, we find that the flow must be a mixture of slip and shear. First, as $n=2$, there are clear signs of correlated shear-induced rearrangements. Second, since we are measuring, for a given $\dot{\gamma} > \dot{\gamma}_S$, smaller $1/T$ than with a rough surface, the foam must still be simultaneously slipping, confirming previous results by [Gopal and Durian \(1995\)](#) on the detection of slip by DWS. So, the true shear rate occurring into the foam must be smaller than the applied one.

If we first consider that the DWS curve for the rough surfaces is ideal (true up to the highest shear rates), and secondly assume that the frequency $1/T$ always reflects the actual shear rate in the bulk, we can recover the real shear rate occurring in the smooth plate case. In that respect, the DWS measurements provide us with the rate at which bubbles are actually sheared within the foam, independently of some possible slip. For instance, an applied shear rate of 7 s^{-1} for the smooth plate corresponds to a true shear rate of 2 s^{-1} , since those both correspond to the same $1/T$, as shown by the arrow in [Fig. 5](#).

We can then re-plot—for the points above the yield stress—the rheology results of [Fig. 2](#) as a function of the real shear rate encountered by the foam: Once this renormalization is done, the data points for the rough and smooth plates almost collapse ([Fig. 9](#)). However, this collapse is not as perfect as it should be if both the real shear stress and shear rate were correctly extracted from the smooth surface data. In fact, when slip occurs simultaneously with the shear, extracting the true shear stress from the measured torque is not as straightforward as in the standard case (considering no slip and uniform stress in the sample). Here we have used the stress value calculated assuming these assumptions, and this must be one of the origins of the observed discrepancy in [Fig. 9](#).

We can also note that for a full collapse of the data in Fig. 9, one just has to subtract a few Pa from the stress obtained when shear and slip occurs: This is typically the correct range of slip stresses measured in the pure slip regime (see Fig. 2), but it is always smaller than the yield stress. It thus appears that the slip contribution is maximum at the yield stress, and that it decreases at higher shear rates. This is actually confirmed by the DWS measurements: Using the renormalization we can deduce the slip velocity. It reaches a maximum at the yield stress, and tends to remain constant (or to slightly decrease) above $\dot{\gamma}_s$. Such behavior is also consistent with observations in [Meeker *et al.* (2004b)] and remains to be fully understood.

B. Slip regime: Comparing data and further quantitative analysis

Our data confirm that the slip regime properties—both exponent and prefactor of the scaling law—depend on the interfacial properties and on the liquid volume fraction. As already stated, many theoretical works have been performed on this topic, and the results mostly dealt with the scaling exponent. The main issue is thus to discuss the quantitative aspects of the problem, in order to converge on a complete model.

First, for comparisons to previous works, we introduce nondimensional quantities allowing us to simplify the dependence with the bubble size, the surface tension and the bulk viscosity. The shear stress τ is normalized by (σ/R) , and in the following we use $\tau' = \tau/(\sigma/R)$ and a capillary number $Ca = \eta V/\sigma$, where η is the surfactant solution viscosity and V is the linear velocity of the foam at the plate surface. The latter is calculated at half the cone radius from the angular velocity, first because this gives the mean linear velocity, and second because it is where the DWS data are collected. Second, for a detailed quantitative analysis, one also has to carefully derive the value of the stress from the measured torque: When pure slip occurs, the stress varies with the cell radius as it depends on the slip velocity. It is found that the standard calculation, which assumes a uniform stress over the sample, remains valid for all the qualitative descriptions in terms of exponent, when a power law relationship between the measured torque and the slip velocity is found [Denkov *et al.* (2005)]. But it can no longer be used and a correction has to be made to determine quantitatively the dimensionless prefactor α'_s defined by $\tau' = \alpha'_s Ca^\delta$ in case of pure slip. Consequently, we have used the formalism described in Denkov *et al.* (2005) to accurately calculate the slip stress (by integrating along a radius) and this prefactor α'_s and the results are given in Fig. 4, right.

Denkov *et al.* (2006) showed that, for “immobile” (or rigid-like) gas–liquid interfaces, the following equation relates the stress needed for slip to the capillary number:

$$\tau' = \tau \left/ \left(\frac{\sigma}{R} \right) \right. = 1.25 C_{I-F} F(\varepsilon) C_a^{1/2} + 2.1 C_{I-PB} H(\varepsilon) C_a^{2/3} \quad (3)$$

With

$$F(\varepsilon) = \frac{f^{3/4}}{\sqrt{1-f^{1/2}}} \quad \text{and} \quad H(\varepsilon) = f^{1/2} \quad (4)$$

The function f only depends on ε : $f = 1 - 3.2 [(1-\varepsilon)/\varepsilon + 7.7]^{-1/2}$, an expression derived empirically by Princen (2001). Equation (3) reflects the geometry of the contact between a foam and a wall. There are two different structures in which fluid motion and viscous dissipation can take place: (i) the flat thin film made by the contact between the bubble face and the wall, and (ii) the thick channels separating the bubbles, also called “surface Plateau borders” (named “PB” in the following). These borders have a triangular-like shape, with one of their faces in contact with the wall. In Eq. (3), the first

contribution—in $Ca^{1/2}$, weighted by the prefactor C_{I-F} —corresponds to viscous dissipation inside the flat wetting film. The second—in $Ca^{2/3}$, weighted by the prefactor C_{I-PB} —comes from dissipation inside the PB. The differences in geometry of these two structures are responsible for the different macroscopic behaviors. This scaling in $Ca^{2/3}$ was also found in the pioneering work of Bretherton (1961), who only takes into account the dissipation in the Plateau border.

For “mobile” interfaces (“fluid-like” ones), predictions for the stress are the following:

$$\tau' = \tau \left/ \left(\frac{\sigma}{R} \right) \right. = 3C_{M-PB}H(\varepsilon)C_a^{2/3} \quad \text{with } H(\varepsilon) = f^{1/2} \quad (5)$$

In these conditions, the dissipation in the film is neglected: There is almost no shear in the film as the bubble interface is flowing with the bulk liquid. Only the effects in the PB are taken into account. Recent numerical refinements by Saugey *et al.* (2006) confirm the scaling with the exponent $2/3$; but note that this is true only in a certain range of Ca (for $Ca > 10^{-3}$ the exponent slightly decreases with Ca).

Coupling these different results, we can first notice that the difference between immobile and mobile cases for the dissipation in the PB is simply in the prefactor (which is still not known). One can just expect that the value for immobile surfaces can be higher than for the mobile ones. Also it turns out from Eqs. (3) and (4) that by increasing the liquid content one should change the balance between dissipation in the film and in the PB, and shift from one scaling to the other: From the dependence with ε , the second contribution becomes bigger as ε increases. However, it is not predicted whether it is physically possible to have this second contribution higher than the first one, and at which value of ε , since the prefactors C_{I-F} and C_{I-PB} are not yet known. So an important issue is to find out what are the prefactors to determine the exact balance between the different contributions.

Our data can now be compared to these models, starting with the measured power law exponent δ . For the CAS foams, one expects highly viscoelastic interfaces and thick gelified films: Our results show that the exponent is $\delta \approx 0.32$, below but close to the predictions for immobile interfaces and for dominant dissipation in the contact film [Eq. (3)]. Indeed, this is what is expected, and it is consistent with previous works on foams and on microgels, all having highly viscoelastic interfaces [Denkov *et al.* (2005); Meeker *et al.* (2004a, 2004b)]. On the opposite, the results for SDS foams are also consistent with the interfacial properties: SDS-covered interfaces are expected to be very fluid-like interfaces so a scaling in $Ca^{2/3}$ should be, and is actually observed. In that respect, the results with GCK are quite interesting: As the liquid volume fraction increases, δ shifts from ~ 0.3 to ~ 0.66 . Thus, in agreement with Eq. (3), it is physically feasible to tune the slip regime—and the location of the main dissipation—by changing the liquid volume fraction ε .

To be more quantitative, we now study the dimensionless prefactors α'_s ($\tau' = \alpha'_s Ca^\delta$) as a function of the liquid volume fraction (Fig. 10, left). For CAS and GCK foams with $\varepsilon < 0.25$, the exponent δ is close and can be forced to 0.5, so that we can compare the measured dependence of α'_s with ε to the first term of Eq. (3). In Fig. 10, left, the solid line represents this theoretical dependence using the value for $C_{I-F} = 3.7$, determined at $\varepsilon = 0.1$ in Denkov *et al.* (2006). A good agreement is observed, and the prefactor smoothly decreases with ε . Practically speaking, this tends to prove that we are normalizing our data as in Denkov *et al.* (2006), with the same definition for the capillary number, etc.

For SDS foams, the exponent is $\delta = 0.65$; in this regime, we can also compare the dependence of the nondimensional prefactors α'_s to the predicted dependence of Eq. (5)

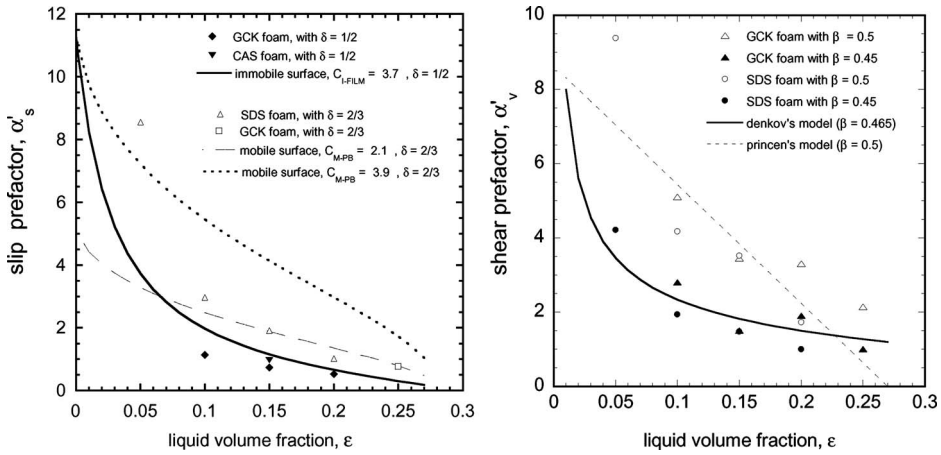


FIG. 10. (Left) Slip regime dimensionless prefactors α'_s as a function of ε , for SDS foams with exponent $\delta = 2/3$ (upright triangles), GCK foams with $\delta = 2/3$ (square), GCK foams with $\delta = 1/2$ (diamond), and CAS foams with $\delta = 1/2$ (downright triangle). The solid line represents the predicted dependency for immobile interfaces with $C_{I-F} = 3.7$, the dotted and dashed lines are the predictions for mobile surfaces with $C_{M-PB} = 3.9$ and $C_{M-PB} = 2.1$, respectively. (Right) Shear regime dimensionless prefactors α'_v as a function of ε , for SDS foams and GCK foams with $\beta = 0.45$ and 0.5 . The lines represent the description from Princen and Kiss (1989) and the model of Denkov *et al.* (2008).

(dotted line in Fig. 10), using the value found by Denkov *et al.* (2005) for $C_{M-PB} = 3.9$ (note that this C_{M-PB} was only inferred from a single measurement at $\varepsilon = 0.1$). We find prefactors about twice smaller than previously reported (except for the point at 0.05 , which appears much higher than the others). Adjusting our data with the model of Eq. (5) provides a rough agreement (dashed line), and a value $C_{M-PB} = 2.1$. Last, we can extract, for the first time, from the GCK point at $\varepsilon = 0.25$ a value for the prefactor C_{I-PB} : the fitting with $\delta = 0.66$ provides $C_{I-PB} = 3.5$. From all these pieces of information, many remarks can be made in order to move towards a complete description of slip. First, with GCK foams, the measured value of C_{I-F} and C_{I-PB} can be plugged into Eq. (3): We consistently find that the second contribution actually becomes dominant for $\varepsilon > 0.2$ (for a typical Ca value).

It is also well confirmed that changing the surfactant changes the slip regime. However, in the Eqs. (3) and (5), such dependencies are not yet included (only the effect of liquid fraction is determined, and fairly validated by data as discussed previously). For a complete and quantitative scheme of slip, one also has to include the effect of the surfactant. In that goal, the slip coefficients (C_{I-F} , etc.) cannot be constant values, but must be functions of the interfacial properties. So, we propose that a complete model for slip must have only two terms, as in Eq. (3). The first one corresponds to dissipation in the film: It depends on the liquid fraction in a way already well described by Eq. (3), and has a prefactor C_{FILM} which is a decreasing function of the interfacial mobility. For perfectly rigid surfaces, $C_{FILM} = C_{I-F}$; for the opposite case of mobile surfaces, C_{FILM} vanishes down to 0, since there is no more contribution of the film in this limit of highly mobile interfaces. For the dissipation in the film, making the surface less and less rigid moves the solid line downwards in Fig. 10, left, the slip stress is lowered (CAS-covered surfaces can be then seen as the limiting case). The second contribution is the one from the PB—scaling in $Ca^{2/3}$ —which depends on the liquid fraction and has a prefactor C_{PB} which is also a decreasing function of the mobility (in order to get higher stresses for more rigid

interfaces). But, oppositely to the case of the film, there is a finite limit for the perfectly mobile case, for which $C_{PB}=3C_{M-PB} \neq 0$. In the other limit of rigid surfaces, the factor $C_{PB}=2.1C_{I-PB}$; note that from our preliminary measurements, it seems that the decrease of the prefactor C_{PB} with the mobility is actually rather small (from $2.1C_{I-PB}=7$ to $3C_{M-PB}=6.3$).

In this global picture, one understands that the second contribution (from the PB) can eventually become dominant as the mobility increases (for any given liquid fraction). As well, for a given surfactant, if one makes dryer foam, the relative contribution of the film will increase.

Our data provide us with the boundary values for the two extreme limits of mobility (with SDS and CAS), and are all consistent with the picture described above. For instance, in this framework, the apparently high value measured for SDS foams at $\varepsilon=0.05$ can be understood by considering that the dissipation in the film can no longer be neglected (because it is in the limit of low ε). Also, the data of [Denkov *et al.* \(2005\)](#) at $\varepsilon=0.1$, from which a higher value of C_{M-PB} has been determined, could be included in this picture, simply by assuming that they correspond to a lower surface mobility than in our case.

The next point is to determine which microscopic interfacial properties are behind the concept of interfacial mobility, and to know if this is related to compression or shear response of the interfaces. On such issues, it might be instructive to consider the analogy between these results and those on foam drainage [[Stone *et al.* \(2003\)](#); [Saint-Jalmes \(2006\)](#)]. In drainage, two opposite regimes are observed, with two different power laws when plotting V vs ε (as here, σ vs Ca). One can change from one regime to the other either by changing the surfactant or the bubble size (as here, with the surfactant and the liquid fraction). The dimensionless prefactors of the power laws are hydrodynamic resistances, which depend on the surface mobility. This mobility includes interfacial properties, liquid fraction and bubble size (as here we have prefactors which also depend on the interfacial properties, the liquid fraction, and the bubble size). Each regime corresponds to a different foam structure in which the dissipation is maximum: “Dissipation in PB” vs “dissipation in nodes” for foam drainage, “dissipation in PB” vs “dissipation in film” for foam slip. In drainage, the relevant interfacial property has been identified as the interfacial shear viscosity: It is the relevant parameter as it describes how the interfaces resist to the bulk flow or are sheared with it. In many ways, the slip issue is similar. Again, the interfacial mobility reflects whether the interfaces are sheared or not by a bulk flow. It is thus quite tempting to propose that the surface shear viscosity could also be the important parameter in this problem of slip, rather than some other shear or compression moduli. But this will have to be assessed in the future.

It is also interesting to discuss quantitatively the slip velocity. Using the DWS data and the rheological curves, we can get the slip velocity V as a function of the foam parameters, especially the maximum value V' . As in [Meeker *et al.* \(2004a, 2004b\)](#) with microgels, we have plotted V' as a function of the quantity GR/η ; G is the shear modulus, measured by small oscillation experiments [[Saint-Jalmes and Durian \(1999b\)](#)]. We find a linear relationship as for the microgels: $V'=kGR/\eta$. Moreover, the factor k is the same ($k=0.003$) and our set of data is well superimposed and implements the previous results (for our foams, the quantity GR/η varies from 1 to 20, while it varies from 10^{-2} to 1 for the microgels, and the typical velocity is about 10–40 mm s⁻¹). To go further, we have seen that the maximum velocity is always obtained for a stress τ equal to the yield stress τ_y . The latter is equal to $\gamma_y G$, where γ_y is the yield strain and G is the elastic shear modulus. Those are decreasing functions of ε : $G=(\sigma/R) \cdot R(\varepsilon)$ and $\gamma_y=\gamma_{y0} \cdot Q(\varepsilon)$ [[Saint-](#)

Jalmes and Durian (1999b)]. When equating the normalized slip and yield stresses, we get for the case of immobile interfaces (viscous dissipation dominating in the films):

$$V' = \frac{\sigma}{\eta} \left[\frac{\gamma_{y0}}{1.25 C_{I-F}} \right]^2 \left[\frac{R(\varepsilon)Q(\varepsilon)}{F(\varepsilon)} \right]^2. \quad (6)$$

And for mobile surfaces (viscous dissipation dominating in the PB):

$$V' = \frac{\sigma}{\eta} \left[\frac{\gamma_{y0}}{3 C_{M-PB}} \right]^{3/2} \left[\frac{R(\varepsilon)Q(\varepsilon)}{H(\varepsilon)} \right]^{3/2} \quad (7)$$

As a matter of fact, the functions $F(\varepsilon)$, $H(\varepsilon)$, $Q(\varepsilon)$, and $R(\varepsilon)$ are quantitatively quite similar; they all decrease slowly with ε , and are typically around 0.3 for $\varepsilon=0.15$. First, this gives some interesting new ways of understanding how the slip prefactor depends on ε [functions $F(\varepsilon)$ and $H(\varepsilon)$] since it seems that there must be some links with how rheological properties depend on ε [functions $R(\varepsilon)$ and $Q(\varepsilon)$]. At a first order, we can assume that RQ/H or $RQ/F \approx 1$. With this simplification and with $\gamma_{y0}=0.2$ [Saint-Jalmes and Durian (1999b)], it follows that we quantitatively calculate both the typical velocity range and the slope k , and that these agree with the measurements ($V' \approx 30$ mm/s and $k=0.003 \pm 0.001$). We have thus been able to explain quantitatively the origin of the slip velocity. Especially, it emphasizes the crucial role of the yield strain value: It is a quantity very similar for many soft materials, and it is thus understandable to get similar results as for microgels. Qualitatively, the results are also consistent with the proposed dependence of the prefactors C_{I-F} and C_{M-PB} with the interfacial properties. If one goes towards rigid interfaces, the values of C_{I-F} and C_{M-PB} increase, and the slip velocity decreases, as expected.

Last, let us comment on the very low shear rates regime seen for GCK, i.e., the occurrence of a plateau for the dryer foams (Fig. 8). Such a “plateau,” which can be seen as a pseudo-yield stress (but still below the real yield stress), has also been observed with microgels [Meeker *et al.* (2004b)]. Though its interpretation is still lacking, it must be related to the facts that, as the foam is dryer, there is more film surface in contact with the wall, smaller PB radius, and that the foam is eventually no longer slipping. As discussed previously for the roughness of a surface, it is the same for the smoothness of a surface: It depends again on the foam properties and the applied deformation, and not only on the surface itself.

C. Shear regime between rough surfaces

With rough surfaces on both sides of the rheometer cell preventing wall slip, the comparison to other systems and to models can also be done. The issues of flow homogeneity and uniformity and the existence of simple universal behavior can thus be investigated. We first notice that once normalized by (σ/R) the measured yield stresses are in agreement with the data reported in the literature [Rouyer *et al.* (2005)]. Then we can look in more detail at the viscous stress, $\tau_v = \tau - \tau_y$. Here again, it can be normalized by (σ/R) and the capillary number Ca can be used. Schwartz and Princen (1987) predicted a scaling regime $\tau_v \sim Ca^\beta$, with $\beta=2/3$ [also found in Reinelt and Kraynik (1989)]; however, it was later found experimentally by Princen that for concentrated emulsions [Princen and Kiss (1989)]:

$$\tau'' = (\tau - \tau_y) \left/ \left(\frac{\sigma}{R} \right) \right. = a(b - \varepsilon) C_a^{1/2}. \quad (8)$$

Similarly, starting from diluted emulsions up to concentrated ones, a shift from $\beta=2/3$ to $\beta=1/2$ (and eventually lower) was also found experimentally [Mason *et al.* (1996)].

More recently, Denkov *et al.* (2005), with rigid and mobile interfaces foams, experimentally found two β , respectively 0.25 ± 0.02 and 0.42 ± 0.02 . A theoretical model based on the calculation of the energy dissipated due to viscous friction inside the films between bubbles has also been proposed by Denkov *et al.* (2008); the viscous stress is then

$$\tau'' = a C_a^\beta (1 - \varepsilon)^{5/6} / \varepsilon^{1/2} \quad (9)$$

with the coefficient $a=0.806$ and the exponent $\beta=0.465$.

Also, with transparent emulsions, an exponent $\beta=0.45$ was found with SDS (at low SDS concentrations, corresponding to nonattractive interactions), and simultaneous measurements of the velocity profile showed that the flow was uniform with this exponent. On the opposite, at higher concentrations of SDS, the interaction between the droplets becomes attractive and the flow is no longer uniform (shear banding occurs).

Experiments on microgels have shown a uniform flow, and an exponent $\beta=0.45$ is also measured. Other experiments showed in one hand that with a same commercial shaving cream there can be shear banding [Bertola *et al.* (2003)] in Couette shear, and in the other hand that rheological data provide an exponent 0.2 (after deducing stress from reported viscosity measurements) [Gopal and Durian (1999)]. Nevertheless, using planar shear geometry, Gopal and Durian came to the conclusion that the flow is uniform in Gillette foams, on the basis of DWS measurements [Gopal and Durian (1995)]. On the side of numerical simulations, recent models on the steady state of sheared glass [Haxton and Liu (2007)] found a β between 0.4 and 0.6, with uniform flows. Last, with extremely dry foams containing SDS, co-surfactants and polymers, some nonlinear velocity profiles have been found [Rouyer *et al.* (2003)].

Compiling all this information, no simple and definitive picture emerges; however, most of the results can be summarized by considering that there are most likely two opposite cases, corresponding to two values of the exponent ($\beta \approx 0.2$ and $\beta \approx 0.45$), and two associated possible types of flow (respectively, with localization or uniform).

Our data are consistent with such previous results, and validate this classification of flow properties. For SDS and GCK foams, the behavior looks very similar to the systems that uniformly flow ($\beta=0.4-0.5$), and is in qualitative agreement with Eq. (9). Oppositely, the CAS foams differ, with a $\beta=0.31 \pm 0.01$, which turns out to be much closer to the one of shaving foams and attractive emulsions. For these foams, it is thus tempting to deduce, by comparisons to other known results, that the flow could be no longer uniform.

So, we show that—as for emulsions—we can get different types of flow depending on the interfacial properties, and it seems one can identify these behaviors thanks to the macroscopic flow curve features. To go further, we can try, as for the slip, to figure out what makes the difference at the microscopic scale between the different regimes. At first sight, a uniform flow might preferentially be found for the simplest chemical formulation, the most fluid-like interfaces and the thinnest films. In that respect, the CAS foams with thick gelled and jammed interstitial films resemble more the attractive emulsions. For such systems, one can qualitatively understand that more energy is required to switch one bubble over another because of the gelified films. Thus, such foams prefer to localize the shear at a given place, rather than everywhere in the sample. Despite that it is likely that the film properties have to play a role, we still lack the relevant quantity, which controls

the shear regime. But, data show also that we must not only consider the interfacial properties: The liquid fraction, as the shearing geometry, must play a role regarding the occurrence of shear localization. Last, to tackle these issues of flow uniformity, it also seems that one has to take into account some nontrivial effects, like dynamic dilatancy, which link the localization of the shear to a liquid fraction gradient [Marze *et al.* (2005)].

Quantitatively, in Fig. 10, right, we compare the results for the prefactors α'_v ($\tau' = \alpha'_v C a^\beta$) to the previous results of Princen and Kiss (1989) and to the recent model of Denkov *et al.* (2008). The comparison to the model of Denkov *et al.* (2008) turns out to be quite correct, both on the exponent as discussed already, but also on this prefactor. The solid line in Fig. 10, right represents the model of Eq. (9). Here, the experimental prefactors are determined by fixing all the β to a same value ($\beta=0.45$) close to the predicted one [Eq. (9)]. It thus seems that this model describes our experimental data well.

If we want to compare our experiments to those of Princen and Kiss (1989), we first have to force $\beta=0.5$, which is less efficient: then one can see that the prefactors α'_v are consistent with the Princen and Kiss (1989) results (dashed line in Fig. 10, right). However, this dashed line does not describe the set of points as well as the solid line. Note also that the experimental result of Denkov *et al.* (2005) at $\varepsilon=0.1$ is very close to the SDS value at $\varepsilon=0.1$ (both with $\beta \approx 0.45$).

On the steady shear, we finally make a few other remarks. First, on the similarity between continuous and oscillation tests, it seems that the results shown in Fig. 3, left show that the Cox–Merz rule holds for foams, at least in the tested cases and ranges of parameters. Here, we did the experiments by controlling the shear rate. But it could be done differently, by controlling the applied stress. With such stress-controlled measurements, a viscosity bifurcation has been observed with shaving foams, as a direct signature of nonuniform flows [Da Cruz (2002); Møller (2006)]. For SDS and GCK foams, our observations tend to show that the flow is uniform, so that there should be no viscosity bifurcation. However, such effects should be seen with CAS foams, as for shaving ones. We are currently performing more experiments in a stress-controlled mode to confirm the consistency of these results.

V. SUMMARY AND CONCLUSIONS

We have reported a large amount of results on steady flows of aqueous foams made of different chemicals, at different liquid fractions, and for different surface roughness. The main contributions we are adding here come first from the fact that we have coupled rheometry and DWS, and second that we have varied the liquid fractions of foams of well-controlled properties. This provided us with a large set of new results at different scales. With such new data and by comparing them to previous works, we have been able to get a better understanding on many issues related to foam slip and shear.

The occurrence of slip at a solid surface is crucial in the mechanical response of the foam: Whether the foam is slipping or not induces quite different behaviors. We have confirmed that there are different slip regimes. Qualitatively, changing the surfactant changes the slip regime. As well, we have experimentally shown that the liquid fraction—for fixed interfacial properties—can also change the slip regime. There are actually two extreme cases, each corresponding to a different location where the viscous dissipation dominates (contact film and PB). In a real situation, viscous dissipations (or resistance) in the film and in the PB are both present, and the balance between them is controlled by the surfactant and the liquid fraction. Quantitatively, we report for the first time experiments showing how the hydrodynamic resistance in the film and in the PB (characterized by C_{FILM} and C_{PB}) depend on the liquid fraction and on the surfactant.

From all our results, we propose that the interfacial properties must be included into these film and PB contributions in such a way that a coefficient C_{FILM} strongly decreases down to 0 with increasing interfacial mobility, whereas C_{PB} must only decrease slightly down to a constant value at high interfacial mobility. These first measurements will help to validate future quantitative models. It remains to determine exactly which microscopic properties of the interface are relevant. From the analogy with drainage and due to the central role of the coupling between bulk and surface flows, we suggest that the shear interfacial viscosity is likely to play this role.

In a more general view, we want to point out that we recover, as in many other aspects of foam physics, that the macroscopic foam properties result from a subtle balance between what is happening in the Plateau borders, the nodes, and the films. Then, by changing the interfacial properties (thus the surfactants used) or the liquid fraction, one can modify the equilibrium between the effects in the different structures, and get different macroscopic behaviors (which significantly differs because the scales and geometries of PB, nodes, and films are quite different).

Thanks to the use of DWS, we have measured the slip velocity, which turns out to have a maximum at the yield stress. In fact, DWS is a very useful tool for discriminating between slipping and sheared foams, and for extracting the real shear rate within the foam. Quantitatively, we have been able to explain the slip velocity; in particular, this analysis enlightens the role of the yield strain of the material.

Concerning the steady shear (without slip), we have first confirmed some previous results, concerning both the dependence of the yield stress and the behavior of the viscous stress with liquid fraction and shear rate. Once the real shear rate is known, we have found that the flow properties depend also on the surfactants. Compiling previous works on emulsions, microgels, and foams, we have been able to determine that our SDS foams most likely flow uniformly, without localization effects, whereas our CAS foams—as the shaving foams—display shear nonuniformities. These results stress the importance of the interaction between bubbles, via the interstitial film properties. But, this remains to be completely elucidated, as well as the balance between such interfacial effects and those of the liquid fraction on the flow uniformity.

We have also brought proofs that steady shear and oscillation measurement modes can provide similar results, tending to show that the Cox–Merz rule holds for foams. Last, these results also show that a surface is never perfectly rough or smooth: It always also depends on the foam properties and the applied shear rate.

ACKNOWLEDGMENTS

The authors thank CNES and ESA (MAP program) for financial support.

References

- Asipauskas, M., M. Aubouy, J. A. Glazier, F. Graner, and Y. Jiang, “A texture tensor to quantify deformations: The example of two-dimensional flowing foams,” *Granular Matter* **5**, 71 (2003).
- Bécu, L., S. Manneville, and A. Colin, “Yielding and flow in adhesive and non adhesive concentrated emulsions,” *Phys. Rev. Lett.* **96**, 138302 (2006).
- Bertola, V., F. Bertrand, H. Tabuteau, D. Bonn, and P. Coussot, “Wall slip and yielding of pasty materials,” *J. Rheol.* **47**, 121 (2003).
- Bos, M. A., and T. van Vliet, “Interfacial rheological properties of adsorbed protein layers and surfactants: A review,” *Adv. Colloid Interface Sci.* **91**, 437 (2001).

- Bretherton, F. P., "The motion of long bubbles in tubes," *J. Fluid Mech.* **10**, 166 (1961).
- Cantat, I., and R. Delannay, "Dissipative flows of 2D foams," *Eur. Phys. J. E* **18**, 55 (2005).
- Cox, S. J., "A viscous froth model for dry foams in the surface evolver," *Colloids Surf., A* **263**, 81 (2006).
- Da Cruz, F., F. Chevoir, D. Bonn, and P. Coussot, "Viscosity bifurcation in granular materials, foams, and emulsions," *Phys. Rev. E* **66**, 051305 (2002).
- Debrégeas, G., H. Tabuteau, and J. M. di Meglio, "Deformation and flow of a two-dimensional foam under continuous shear," *Phys. Rev. Lett.* **87**, 178305 (2001).
- Denkov, N. D., V. Subramanian, D. Gurovich, and A. Lips, "Wall slip and viscous dissipation in sheared foams: Effect of surface mobility," *Colloids Surf., A* **263**, 129 (2005).
- Denkov, N. D., S. Tcholakova, K. Golemanov, V. Subramanian, and A. Lips, "Foam-wall friction: Effect of air volume fraction for tangentially immobile bubble surface," *Colloids Surf., A* **282**, 329 (2006).
- Denkov, N. D., S. Tcholakova, K. Golemanov, K. P. Ananthapadmanabhan, and A. Lips, "Viscous friction in foams and concentrated emulsions under steady shear," *Phys. Rev. Lett.* **100**, 138301 (2008).
- Dollet, B., and F. Graner, "Two-dimensional flow of foam around a circular obstacle: Local measurements of elasticity, plasticity and flow," *J. Fluid Mech.* **585**, 181 (2007).
- Durian, D. J., D. A. Weitz, and D. J. Pine, "Scaling behavior in shaving cream," *Phys. Rev. A* **44**, R7902 (1991).
- Durian, D. J., "Accuracy of diffusing-wave spectroscopy theories," *Phys. Rev. E* **51**, 3350 (1995).
- Emile, J., E. Hardy, E. Terriac, A. Saint-Jalmes, and R. Delannay, "Swelling of a single foam film under slipping," *Colloids Surf., A* **304**, 72 (2007).
- Gopal, A. D., and D. J. Durian, "Non-linear bubble dynamics in a slowly driven foam," *Phys. Rev. Lett.* **75**, 2610 (1995).
- Gopal, A. D., and D. J. Durian, "Shear-induced "melting" of an aqueous foam," *J. Colloid Interface Sci.* **213**, 169 (1999).
- Haxton, T., and A. Liu, "Activated dynamics and effective temperature in a steady state sheared glass," arXiv:0706.0235 (2007).
- Höhler, R., and S. Cohen-Addad, "Rheology of liquid foam," *J. Phys.: Condens. Matter* **17**, R1041 (2005).
- Janiaud, E., and F. Graner, "Foam in a two-dimensional Couette shear: A local measurement of bubble deformation," *J. Fluid Mech.* **532**, 243 (2005).
- Janiaud, E., S. Hutzler, and D. Weaire, "Two dimensional foam rheology with viscous drag," *Phys. Rev. Lett.* **97**, 038302 (2006).
- Khan, S. A., C. A. Schnepper, and R. C. Armstrong, "Foam rheology: III. Measurement of shear flow properties," *J. Rheol.* **32**, 69 (1988).
- Kraynik, A. M., D. A. Reinelt, and H. M. Princen, "The non-linear elastic behavior of polydisperse hexagonal foams and concentrated emulsions," *J. Rheol.* **35**, 1235 (1991).
- Marze, S., A. Saint-Jalmes, and D. Langevin, "Protein and surfactant foams: Linear rheology and dilatancy effects," *Colloids Surf., A* **263**, 121 (2005).
- Mason, T. G., J. Bibette, and D. A. Weitz, "Yielding and flow of monodisperse emulsions," *J. Colloid Interface Sci.* **179**, 439 (1996).
- Meeker, S. P., R. T. Bonnecaze, and M. Cloitre, "Slip and flow of soft particles pastes," *Phys. Rev. Lett.* **92**, 198302 (2004a).
- Meeker, S. P., R. T. Bonnecaze, and M. Cloitre, "Slip and flow of soft particles: Direct observation and rheology," *J. Rheol.* **48**(6), 1295 (2004b).
- Møller, P. C. F., J. Mewis, and D. Bonn, "Yield stress and thixotropy: On the difficulty of measuring yield stresses in practice," *Soft Matter* **2**, 274 (2006).
- Princen, H. M., and A. D. Kiss, "Rheology of foams and highly concentrated emulsions. IV: An experimental study of the shear viscosity and yield stress of concentrated emulsions," *J. Colloid Interface Sci.* **128**, 176 (1989).
- Princen, H. M., *Encyclopedia of Emulsion Technology*, edited by J. Stöblom (Dekker, New York, 2001), Chap. 11, p. 243.
- Raynaud, J. S., P. Moucheront, J. C. Baudez, F. Bertrand, J. P. Guilbaud, and P. Coussot, "Direct determination by NMR of the thixotropic and yielding behavior of suspensions," *J. Rheol.* **46**, 709 (2002).

- Reinelt, D. A., and A. M. Kraynik, "Viscous effects in the rheology of foams and concentrated emulsions," *J. Colloid Interface Sci.* **132**, 491 (1989).
- Reinelt, D. A., and A. M. Kraynik, "Large elastic deformations of three-dimensional foams and highly concentrated emulsions," *J. Colloid Interface Sci.* **159**, 460 (1993).
- Rodts, S., J. C. Baudez, and P. Coussot, "From discrete to continuum flow in foams," *Europhys. Lett.* **69**, 636 (2005).
- Rouyer, F., S. Cohen-Addad, and R. Höhler, "Dynamics of yielding observed in a three dimensional aqueous dry foam," *Phys. Rev. E* **67**, 021405 (2003).
- Rouyer, F., S. Cohen-Addad, and R. Höhler, "Is the yield stress of aqueous foam a well-defined quantity?," *Colloids Surf., A* **263**, 111 (2005).
- Saint-Jalmes, A., M. U. Vera, and D. J. Durian, "Uniform foam production by turbulent mixing: New results on free drainage vs. liquid content," *Eur. Phys. J. B* **12**, 67 (1999a).
- Saint-Jalmes, A., and D. J. Durian, "Vanishing elasticity for wet foams: Equivalence with emulsions and role of polydispersity," *J. Rheol.* **43**, 1411 (1999b).
- Saint-Jalmes, A., M. L. Peugeot, H. Ferraz, and D. Langevin, "Differences between protein and surfactant foams: Microscopic properties, stability and coarsening," *Colloids Surf., A* **263**, 219 (2005).
- Saint-Jalmes, A., "Physical-chemistry in foam drainage and coarsening," *Soft Matter* **2**, 836 (2006).
- Saugey, A., W. Drenckhan, and D. Weaire, "Wall slip of bubbles in foams," *Phys. Fluids* **18**, 053101 (2006).
- Schwartz, L. W., and H. M. Princen, "A theory of extensional viscosity for flowing foams and concentrated emulsions," *J. Colloid Interface Sci.* **118**, 201 (1987).
- Stone, H. A., S. A. Koehler, S. Hilgenfeldt, and M. Durand, "Perspectives on foam drainage and the influence of interfacial rheology," *J. Phys.: Condens. Matter* **15**, S283 (2003).
- Terriac, E., J. Etrillard, and I. Cantat, "Viscous forces exerted on a foam at a solid boundary: Influence of the liquid fraction and of the bubble size," *Europhys. Lett.* **74**, 909 (2006).
- Tewari, S., D. Schiemann, D. J. Durian, C. M. Knobler, S. A. Langer, and A. J. Liu, "Statistics of shear induced rearrangements in a two-dimensional model foam," *Phys. Rev. E* **60**, 4385 (1999).
- Vera, M. U., A. Saint-Jalmes, and D. J. Durian, "Scattering optics of foam," *Appl. Opt.* **40**, 4210 (2001).
- Wang, Y., K. Krishan, and M. Dennin, "Impact of boundaries on velocity profiles in bubble raft," *Phys. Rev. E* **73**, 031401 (2006).
- Weitz, D. A., and D. J. Pine, "Diffusing-wave spectroscopy," *Dynamic Light Scattering: The Method and Some Applications*, edited by W. Brown (Clarendon, Oxford, 1993), Chap. 16, p. 652.
- Wu, X. L., D. J. Pine, P. M. Chaikin, J. S. Huang, and D. A. Weitz, "Diffusing-wave spectroscopy in a shear flow," *J. Opt. Soc. Am. B* **7**, 15 (1990).